IL NUOVO CIMENTO Vol. 37 C, N. 4 Luglio-Agosto 2014
DOI 10.1393/ncc/i2014-11797-y

Communications: SIF Congress 2013

Neutrinoless double beta decay in GERDA Phase II

C. Macolino(*) on behalf of the GERDA Collaboration
INFN, LNGS, Laboratori Nazionali del Gran Sasso - Assergi (AQ), Italy

ricevuto il 24 Febbraio 2014; approvato il 28 Febbraio 2014

Summary. — The GERmanium Detector Array, GERDA, is designed to search for neutrinoless double beta ($0\nu\beta\beta$) decay of ^{76}Ge and it is installed in the Laboratori Nazionali del Gran Sasso (LNGS) of INFN, Italy. The GERDA experiment has completed the Phase I with a total collected exposure of 21.6 kg yr and a background index (BI) of the order of BI $\simeq 10^{-2}$ cts/(keV kg yr). No excess of events from $0\nu\beta\beta$ decay has been observed and a lower limit on the half-life on the $0\nu\beta\beta$ decay for ^{76}Ge has been estimated: $T^{0\nu}_{1/2} > 2.1 \cdot 10^{25}$ yr at 90% CL. The goal of GERDA Phase II is to reach the target sensitivity of $T^{0\nu}_{1/2} \simeq 1.4 \cdot 10^{26}$ yr, with an increased total mass of the enriched material and a reduced background level. In this paper the results from GERDA Phase I and the major improvements planned for Phase II are discussed.

PACS 14.60.Pq – Neutrino mass and mixing.
PACS 23.40.-s – β decay; double β decay; electron and muon capture.

1. – Introduction

Neutrinoless double beta decay ($0\nu\beta\beta$) gives direct information on the possible "Majorana" nature of the neutrino, *i.e.* when each neutrino eigenstate ν_i coincides with its antiparticle $\bar{\nu}_i$. The observation of such decay would establish lepton number violation and physics beyond the Standard Model would be required. Additionally, neutrinoless double beta decay could give an indirect measurement on the absolute mass of neutrino and shed light to the hierarchy of neutrino masses.

Two-neutrino double beta decay ($2\nu\beta\beta$), *e.g.*

$$(A, Z) \rightarrow (A, Z+2) + 2e^- + 2\bar{\nu}_e, \tag{1}$$

is a second-order process allowed within the Standard Model and that can be observed for some even-even nuclei when ordinary beta decay is energetically prohibited. Neutrinoless

(*) E-mail: carla.macolino@lngs.infn.it

double beta decay ($0\nu\beta\beta$) is not allowed within the Standard Model and can occur only if the neutrino has a non-zero mass and is a Majorana particle. Some theoretical models predict that $0\nu\beta\beta$ could be mediated by a light Majorana neutrino. In this case the effective Majorana neutrino mass is related to the half-life of the decay via the following relation:

$$\frac{1}{T^{0\nu}_{1/2}(A,Z)} = F^{0\nu} \cdot |\mathcal{M}^{0\nu}|^2 \cdot \left|\frac{m_{\beta\beta}}{m_e}\right|^2, \tag{2}$$

where m_e is the electron mass, $F^{0\nu}$ is the phase space factor, $\mathcal{M}^{0\nu}$ is the nuclear matrix element (NME) and $m_{\beta\beta}$ is the effective Majorana electron neutrino mass:

$$m_{\beta\beta} \equiv |U_{e1}|^2 m_1 + |U_{e2}|^2 m_2 e^{i\phi_2} + |U_{e3}|^2 m_3 e^{i\phi_3}, \tag{3}$$

where m_i are the masses of the neutrino mass eigenstates, U_{ei} the elements of the neutrino mixing matrix and $e^{i\phi_2}$ and $e^{i\phi_3}$ the relative Majorana CP phase factors.

The experimental signature for $0\nu\beta\beta$ decay is the observation of a narrow peak at the end-point of the $2\nu\beta\beta$ decay energy spectrum, corresponding to the Q-value ($Q_{\beta\beta}$) of the decay. The number of counts in the peak would allow to quantify the decay rate of the process or, in case of no signal, to set a lower limit on it, via the relation

$$T^{0\nu}_{1/2} = \frac{\ln 2 \cdot N_A}{N^{0\nu}} \cdot \varepsilon \cdot \epsilon \cdot \frac{k}{M_A} \tag{4}$$

with N_A the Avogradro's number, ε the total exposure (detector mass $\times$ live time), ϵ the detection efficiency, k the enrichment fraction of the enriched material (k corresponds to the fraction of ^{76}Ge atoms (f_{76}) in GERDA detectors) and M_A the molar mass of the enriched material (75.6 g GERDA detectors). $N^{0\nu}$ is the observed signal strength or the corresponding upper limit.

The GERDA experiment [1,2] searches for neutrinoless double beta decay of ^{76}Ge, in which ^{76}Ge ($Z = 32$) would decay into ^{76}Se ($Z = 34$) and two electrons. The detectors employed in the GERDA setup are germanium semiconductors with an isotope fraction of ^{76}Ge enriched to about 86% (^{enr}Ge) and which act as both the decay source and a 4π detector. The very good energy resolution of the detectors allows a clear distinction of the neutrinoless double beta peak at $Q_{\beta\beta} = 2039\,\text{keV}$.

Prior to the latest GERDA result, the best limits for $0\nu\beta\beta$ decay in ^{76}Ge were provided by the Heidelberg-Moscow (HdM) [3] and IGEX [4] enriched ^{76}Ge experiments, that yielded lower half-life limits of $T_{1/2} > 1.9 \cdot 10^{25}\,\text{yr}$ and $T_{1/2} > 1.6 \cdot 10^{25}\,\text{yr}$, respectively, corresponding to an upper limit on the effective Majorana mass of $m_{\beta\beta} < 0.33$–$1.35\,\text{eV}$ (the range in mass arises from the differences in models for the estimation of the nuclear matrix element). A subgroup of the HdM Collaboration claimed the observation of 28.75 ± 6.86 $0\nu\beta\beta$ decay events; this translates in a half-life of $T^{0\nu}_{1/2} = 1.19^{+0.37}_{-0.23} \cdot 10^{25}\,\text{yr}$, corresponding to a range for $m_{\beta\beta}$ between 0.24 and 0.58 eV, with a central value of 0.44 eV [5]. In a more sophisticated analysis, the authors found a value for the half-life $T^{0\nu}_{1/2} = 2.23^{+0.44}_{-0.31} \cdot 10^{25}\,\text{yr}$ [6], but some inconsistencies associated to this result have been pointed out in ref. [7]. Other results have been recently published by Kamland-Zen [8] and EXO-200 [9], reporting 90% CL half-life limits for $0\nu\beta\beta$ decay of ^{136}Xe equal to $1.9 \cdot 10^{25}\,\text{yr}$ and $1.6 \cdot 10^{25}\,\text{yr}$, respectively. Nuclear matrix element calculations are

Fig. 1. – An artist's view of the GERDA detector. The array of Ge detectors is not to scale. (1): the array of germanium detector string; (2): the stainless-steel cryostat; (3): the radon shroud; (4): the water tank; (5): the clean room; (6): the insertion lock. Plot from ref. [11].

needed to relate these results to the claim for ^{76}Ge while for GERDA the comparision is straightforward since the same isotope is used.

The aim of GERDA Phase I was to verify the previous results and to reach a much higher sensitivity than previous experiments. The first result on $0\nu\beta\beta$ decay is published in ref. [10]. The plan for GERDA Phase II is to reach the target sensitivity of about $T^{0\nu}_{1/2} \simeq 1.4 \cdot 10^{26}$ yr, with an increased total mass of the enriched material and a reduced background level. The outline of the paper is the following: the experimental setup and the data selection of GERDA are described in sect. **2**; the main result concerning $0\nu\beta\beta$ decay is discussed in sect. **3**. Finally, the major improvements planned for the Phase II of the experiments are discussed in sect. **4**.

2. – The GERDA experiment

GERDA operates an array of bare ^{enr}Ge (Ge detectors enriched in ^{76}Ge) detectors, placed in strings in a cryostat containing liquid argon (LAr) and surrounded by an additional shield of ultra-pure water. Liquid argon acts both as cooling medium for the ^{enr}Ge detectors and shield against external gamma radiation [11]. In fig. 1 an artist's view of the GERDA detector is shown. The cryostat is a steel vessel of 4 m diameter with a copper lining, to reduce gamma radiation from the steel vessel. To prevent radon emanation from the vessel walls and convection close the Ge diodes, the central volume is separated from the rest of the cryostat by a 3 m high and 750 mm diameter cylinder, made of a 30 μm copper foil ("radon shroud"). The cryostat is surrounded by a large tank (8.5 m high and 10 m of diameter) containing ultra-pure water, which corresponds to a 3 m thick water buffer around the cryostat. The water buffer has different purposes; it is used to: i) moderate and absorb neutrons, ii) attenuate the flux of external γ radiation, iii) provide the Cherenkov medium for the detection of muons and iv) provide a backup system for warming up the argon gas in case of emergency. To easily insert the detector strings and the calibration sources into the cryostat, without increasing the contamination of the cryogenic volume, a cleanroom and a lock are located on top of

the vessel. The water tank is instrumented with 66 PMTs, to detect Cherenkov light produced by muon induced showers in the water buffer. An array of 36 plastic scintillator panels is placed on the top of the roof of the cleanroom. Cherenkov and scintillation signals are combined as a muon veto for the data acquisition according to a logic OR. For further details about the GERDA experimental setup see ref. [11].

Data acquisition of GERDA Phase I started on November, 2011 with 8 p-type ^{enr}Ge semi-coaxial (HPGe) detectors, 4 coming from the previous HdM experiment, 1 not enriched from the GENIUS-Test-Facility [12] and 3 from the IGEX experiment, with a total mass of about 20.7 kg (17.7 kg enriched and 3 kg not enriched). On July 2012, 5 Broad Energy GErmanium diodes (manufactured in Olen, Belgium by Canberra), BEGes, with total mass of about 3.6 kg and foreseen for the Phase II of the experiment, were also deployed, in order to test them in a realistic environment. The detector array has a structure made of individual strings, each of them containing up to five independent Ge detectors. In the very first phase of GERDA data taking, a very high background was observed ($18 \cdot 10^{-2}$ cts/(keV kg yr)) and the line at 1525 keV from ^{42}K, the progeny of ^{42}Ar, had an intensity in the energy spectrum much higher than expected [13]. These observations suggested the hypothesis that charged ions of ^{42}K drifted in the electric field produced by the 3 to 4 kV bias of the bare Ge diodes. For this reason the strings of detectors were enclosed into 60 μm thick copper cylinders ("mini-shrouds").

Signals from each detector are read out by a charge sensitive amplifier at about 30 cm from the detectors. The signal is then digitized by 100 MHz Flash ADCs. Digital filters reconstruct the physical parameters as the energy and the risetime of the event. Noise events are identified and rejected by a software algorithm [14]. No real event with energy deposition between 1.3 and 2.7 MeV was rejected and no unphysical event was kept among GERDA Phase I data. The energy deposition of real $0\nu\beta\beta$ decays occurs in only one detector; events with energy deposition in more than one detector or in time correlation (within 8 μs) with a signal from the muon veto are rejected. Possible background events from the ^{214}Bi-^{214}Po decay chain are also rejected, by requiring a time difference of more that 1 ms between one event and the successive one. The energy scale is determined by calibrating the detectors with ^{228}Th sources on a weekly basis. The exposure-weighted average energy resolution (FWHM), extrapolated at $Q_{\beta\beta}$, is (4.8 ± 0.2) keV for semi-coaxial detectors and (3.2 ± 0.2) keV for BEGes. The fitted resolution was stable during the entire data acquisition period. Indeed, the differences between the reconstructed peaks of the ^{228}Th spectrum and the ones from the calibration curves are smaller than 0.3 keV.

Events in the interval $Q_{\beta\beta} \pm 20$ keV were "blinded", *i.e.* they were not processed until the calibration was finalized and all the selection cuts and analyses were fixed.

The experimental energy spectra for the enriched and natural detectors are shown in fig. 2. The green boxes indicate the blinded window of 20 keV around the $Q_{\beta\beta}$ value. There are visible gamma peaks from ^{40}K and ^{42}K decays and from the decay chains of ^{226}Ra and ^{232}Th. The low energy part of the spectrum is dominated by the β decay of ^{39}Ar which has an endpoint of 565 keV. Events from $2\nu\beta\beta$ decay in the range from 600 to 1400 keV are also clearly visible in the spectrum. At energies above 4000 keV a background contribution from α decay of ^{210}Po and ^{226}Ra decay chain is dominant. The half-life of $2\nu\beta\beta$ decay for ^{76}Ge has been measured with a fit to the experimental spectrum between 600 and 1800 keV (see ref. [15]).

The energy spectrum from semi-coaxial and BEGe detectors is fitted to a background model in the energy range between 570 and 7500 keV (for further details see ref. [16]). The contamination contributions were simulated to be located into different hardware

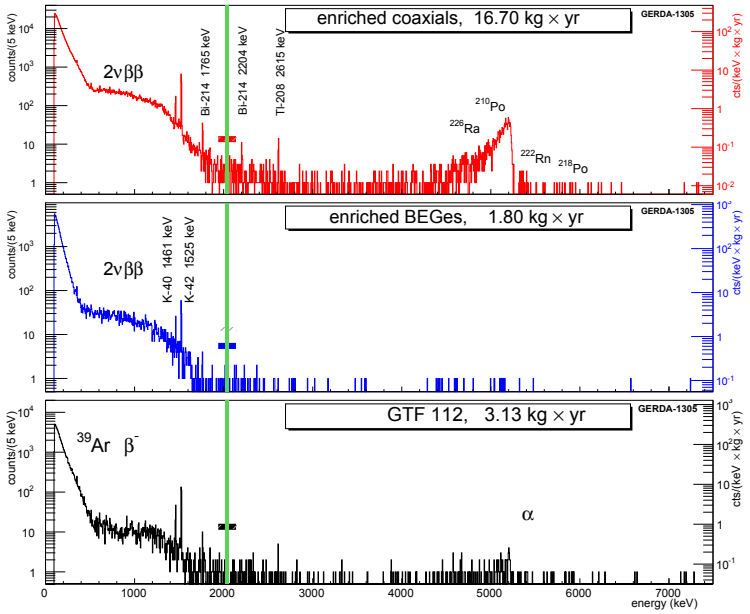

Fig. 2. – Spectra from enriched semi-coaxial (top), enriched BEGe (middle) and non-enriched (bottom) detectors of GERDA Phase I. The green line indicates the $Q_{\beta\beta} \pm 20\,\mathrm{keV}$ region of blinded data. The y-axis scale on the right-hand side indicates the corresponding background index. Plots from ref. [16].

components of the detector setup. Two global models were obtained through a Bayesian fit of the simulated energy spectrum to the measured one: a "minimum model" fit, were only a minimum amount of background components were considered, and a "maximum model" fit, containing all the possible contributions. In the "minimum model" only background sources located close to the detectors (up to 2 cm), were considered. In the "maximum model" further medium and large distance background components were added to the model. Once fitted the models to the data, the result was used to derive the activities of the different background contributions. It turns out that data are well described by both models and that there is no unique determination of the count rates of the different background components. However, the largest fraction of background around comes from sources close to the detectors or on the detector surfaces and no peak is expected to appear in a $\pm 20\,\mathrm{keV}$ window around $Q_{\beta\beta}$. Indeed, the background can be well approximated by a constant in the energy window from 1930 to 2190 keV, with the exclusion of the $\pm 5\,\mathrm{keV}$ regions around the position of γ lines, (single escape peak from ^{208}Tl at 2104 keV and γ line at 2119 keV from ^{214}Bi). The experimental spectrum and the "minimum model" fit are shown in fig. 3, where the considered background contributions are also shown. The background model and the extrapolated value of a fit to the experimental data in a 200 keV energy window into the blinded energy window are in agreement. The interpolated value for BI is BI $= 1.75^{+0.26}_{-0.24} \times 10^{-2}\,\mathrm{cts/(keV\,kg\,yr)}$ for semi-coaxial detectors and BI $= 3.6^{+1.3}_{-1.0} \times 10^{-2}\,\mathrm{cts/(keV\,kg\,yr)}$ for the BEGe detectors.

In GERDA detectors $0\nu\beta\beta$ events have a peculiar pulse shape which can be used to discriminate them from background events: if bremsstrahlung energy loss of electrons in

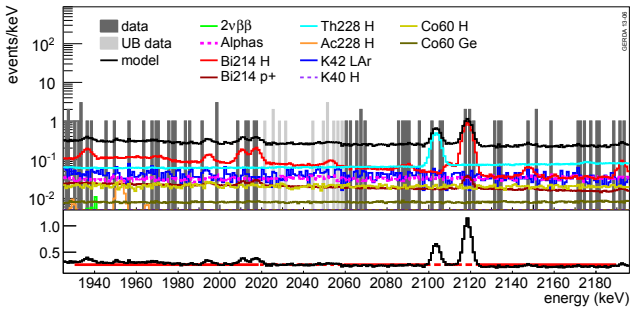

Fig. 3. – Experimental energy spectrum from semi-coaxial enriched detectors around $Q_{\beta\beta}$ and the background decomposition with different possible contributions. The labels for the location mean p^+ on p^+ detector surface, H close to the detector, *e.g.* on the holder, LAr homogeneous in the argon, Ge inside the Ge detectors. The interval of 20 keV around $Q_{\beta\beta}$ was blinded and not used for the fit. The light grey histogram shows a partially unblinded interval. Plot from ref. [16].

$0\nu\beta\beta$ events is small, the two electrons deposit their energy via ionization at one location in the detector and therefore are called Single Site Events (SSE). Conversely, the background is mostly due to γ events and their energy is deposited at multiple locations in the detectors, via multiple Compton scatterings; γ's can, indeed, travel several centimeters. These events are called Multi Site Events (MSE). The discrimination of $0\nu\beta\beta$ events, based on the shape of the recorded pulses, is called Pulse Shape Discrimination (PSD). In GERDA Phase I two different methods for PSD are used, according to the different characteristics of the pulses and electric field distributions of semi-coaxial and BEGe detectors [17].

3. – Results on neutrinoless double beta decay of ^{76}Ge

A limit on the half-life of $0\nu\beta\beta$ decay in ^{76}Ge was derived with the total collected exposure of GERDA Phase I data, *i.e.* 21.6 kg yr (see refs. [10] and [18]). The data are divided into three sets, one containing the BEGe data (called "BEGe" set), one containing data from semi-coaxial detectors with higher background index corresponding at the time when the BEGe detectors were deployed ("silver" set) and, finally, one containing semi-coaxial data except "silver" data (labelled as "golden" set). After the analysis cuts and methods were fixed, events in the blinded window were processed. In the $Q_{\beta\beta} \pm 5$ keV range the background appears flat and seven events are observed while 5.1 ± 0.5 are expected from background counts. After the PSD cut, three of the six events from the semi-coaxial detectors and the one from the BEGe detector are classified as background. In fig. 4 the spectrum before and after PSD is shown, together with the likelihood fit and the expectation based on the claim from ref. [5]. No event remains in the energy window $Q_{\beta\beta} \pm \sigma_E$. The half-life on the $0\nu\beta\beta$ decay was calculated according to eq. (4). For GERDA, the efficiency factor ϵ contains the following terms:

$$\epsilon = f_{av} \cdot \epsilon_{fep} \cdot \epsilon_{psd}, \tag{5}$$

where f_{av} is the active volume fraction, ϵ_{fep} is the probability for a $0\nu\beta\beta$ decay to release its entire energy into the active volume and ϵ_{psd} is the efficiency of the PSD analysis.

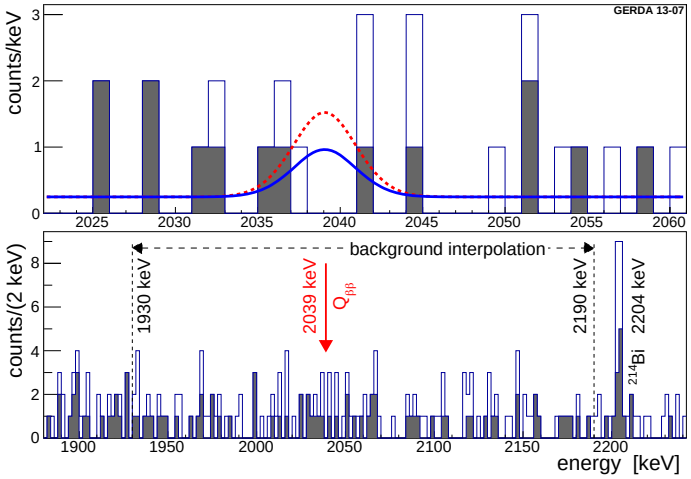

Fig. 4. – Energy spectrum from all ^{enr}Ge detectors with (filled) and without (open) the PSD selection. In the upper panel the expectation based on the central value of the half-life predicted by ref. [5] is also shown (red), together with the 90% CL limit predicted by GERDA Phase I (blue). In the lower panel the energy window used for the backgrund interpolation is indicated. Plot from ref. [10].

The analysis to derive the signal strength was performed according to a profile likelihood fit on the three GERDA data sets. The fitted function contains three constant terms for the background coming from the three data sets and a Gaussian peak, centered at $Q_{\beta\beta}$ and with standard deviation according to the energy resolution (FWHM). The four corresponding parameters of the function were the three terms for the background and $1/T^{0\nu}_{1/2}$, the latter being proportional to the peak counts (see eq. (4)) and common to the three subsets. The best-fit value obtained was $N^{0\nu} = 0$ pointing out that no excess above background was found. The limit on the half-life is

$$T^{0\nu}_{1/2} > 2.1 \cdot 10^{25}\,\mathrm{yr} \quad (90\%\ \mathrm{CL}). \tag{6}$$

The systematic uncertainties due to detector parameters, selection efficiency, energy resolution and energy scale, were folded (by Monte Carlo simulations) into the half-life estimation; they weaken the limit by about 1.5%. The corresponding limit on the number of signal events is $N^{0\nu} < 3.5$ counts. The median sensitivity for the 90% CL limit, given the background levels and the efficiencies, is $T^{0\nu}_{1/2} > 2.4 \cdot 10^{25}$ yr. A Bayesian analysis [19] was also performed (using the BAT toolkit [20]) with the same fit and a flat prior distribution for $1/T^{0\nu}_{1/2}$ between 0 and $10^{-24}\,\mathrm{yr}^{-1}$. The corresponding result for the limit on the half-life is $T^{0\nu}_{1/2} > 1.9 \cdot 10^{25}$ yr, with a median sensitivity of $T^{0\nu}_{1/2} > 2.0 \cdot 10^{25}$ yr. The GERDA result does not support the previous claim of $0\nu\beta\beta$ decay observation in ^{76}Ge [5]. The Bayes factor, *i.e.* the ratio between the probability that the observed data D are produced under the assumption of the model H_1 ($0\nu\beta\beta$ with half-life $T^{0\nu}_{1/2}$ from ref. [5]) and the probability that they are produced under the assumption of the model H_0 (only background), is $P(D|H_1)/P(D|H_0) = 0.024$.

A combined profile likelihood considering GERDA data, together with data from the previous HdM [3] and IGEX [4] experiments, gives again $N^{0\nu} = 0$ as best fit and

$$T^{0\nu}_{1/2} > 3.0 \cdot 10^{25}\,\text{yr} \quad (90\%\ \text{CL}). \tag{7}$$

A Bayesian analysis gives the same limit and Bayes factor equal to $P(D|H_1)/P(D|H_0) = 2 \cdot 10^{-4}$. Results from ^{76}Ge experiments are also compared to the recent limits from KamLAND-Zen [8] and EXO-200 [9] on ^{136}Xe half-life, by rescaling the value of the half-life by the square of the ratio between the nuclear matrix elements $M_{0\nu}(^{76}\text{Ge})/M_{0\nu}(^{136}\text{Xe})$. Considering the most conservative value for the NME [28, 29] of those listed in ref. [21], the Bayes Factor obtained by this combination is 0.0022. The claim is again strongly disfavoured. Considering the most recent value for the ^{76}Ge phase-space factor [22] and the NME calculations reported in references. From [23-29] (scaling the different g_A and R_A parameters according to ref. [30]), the derived upper limits on the effective electron neutrino mass range between 0.2 and 0.4 eV.

4. – Phase II upgrades

The main goal of GERDA Phase II is to get a lower background level and a larger exposure with respect to Phase I. To achieve this goal some upgrades are required, consisting in a scintillation veto from LAr and the procurement of 30 additional enriched BEGe detectors, so to get a total mass of about 35 kg.

The LAr instrumentation permits to detect the 128 nm scintillation light generated in liquid argon by radioactive background decays or cosmic muons. Indeed these decays can occur either in liquid argon or in the detectors, with the emission of gamma particles which eventually excite the argon. The scintillation light has to be shifted to higher wavelength to be detected. There are three different detection setups under investigation for GERDA Phase II. The first design considers PMTs on top and bottom of the detector array, to detect light shifted and reflected on a shroud surrounding the strings; in addition to that, light is also directly detected by PMTs coated by wavelength shifter. In this case two different types of shroud are under consideration, the first made of transparent nylon and the second made of meshed copper. The second design is based on the use of a curtain made of light-guiding fibers all around the detector strings. The light from the fibers is read out by Silicon Photo-Multipliers (SiPMs) on the top of the array. The third solution consists in the use of the Cu foil mini-shroud already implemented in Phase I, which is opaque to light (see fig. 5). In this last case, scintillation light is detected by large-area SiPMs placed in the vicinity of the detectors inside the mini-shroud. The capability to reduce the background by the LAr veto was already demonstrated in the GERDA R&D facility LArGe, where the suppression factors for internal sources of ^{228}Th and ^{214}Bi in around the $Q_{\beta\beta}$ were up to 1180 and 4.6, respectively. The choice of the best setup for the veto will be made according to the solution which will provide the higher suppression for the ^{42}K contamination, the higher background source for GERDA Phase II. In addition, residual background contamination will be rejected by the Pulse Shape Discrimination, as described in ref. [17]. Indeed, ^{42}K contamination is well rejected by the cut based on the PSD qualifier (A/E value) for BEGes. This is shown in fig. 6, where physics data within 200 keV of $Q_{\beta\beta}$ are compared to simulations of ^{42}K decays at the n^+ electrode surface. An even better rejection of such contamination is still possible, paying the price of lowering the selection efficiency for single site events. The estimation

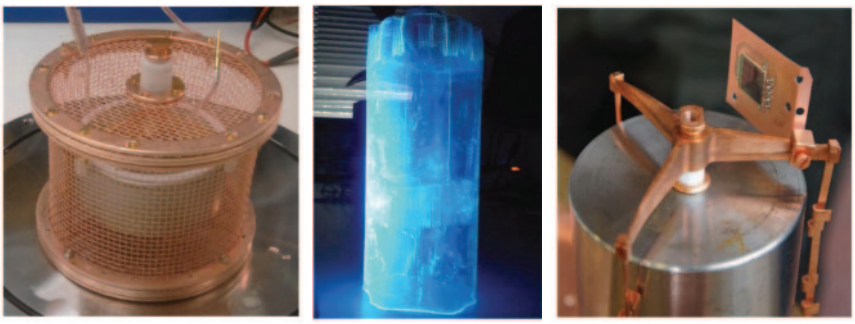

Fig. 5. – The three different options for the mini-shroud around the Ge detector strings: (a) the meshed Cu mini-shroud; (b) the nylon mini-shroud; (c) the BEGe detector with the SiPM. In this last case both the detector and the SiPM are enclosed by the Cu mini-shroud from Phase I.

of the expected background index for GERDA Phase II, when the combination of LAr veto and Pulse Shape Discrimination is used, is of the order of 10^{-3} cts/(keV kg yr).

Enriched germanium procurement and BEGe detectors production has been made under the organization of the GERDA Collaboration. The complete production chain was tested with the use of five BEGes depleted in ^{76}Ge [31], a residual from the enrichment process. During the production chain exposure to cosmic rays was minimized to few days per detector and their transportation was performed in a shipping container passively shielded with about 20 ton of steel and water. The storage and the characterization of the detectors was made in underground locations. The germanium was enriched in the Electrochemical Plant Zelenogorsk (Russia) and zone-refined by PPM Pure Metals GmbH Langelsheim (Germany). The crystals where pulled at Canberra Oak Ridge (USA) and in the end the diodes were produced at Canberra Olen (Belgium). During the production of the diodes an acceptance test campaign was performed by GERDA collaborators in the HADES underground facility of SCK·CEN in Mol, Belgium [32]. The Phase II detectors

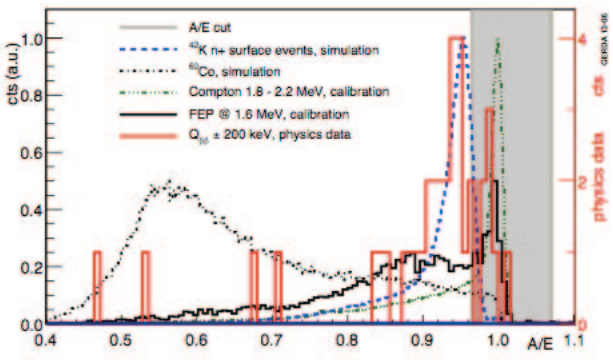

Fig. 6. – PSD qualifier (called A/E) histogram of experimental data from BEGe detectors within 200 keV around $Q_{\beta\beta}$. Result from data is compared to Compton continuum events (green dot-dot dashed), 1621 FEP events (black) from calibration data, simulations of ^{42}K decays at the n^+ electrode surface (blue dashed) and ^{60}Co decay (black dot-dashed). The accepted interval is shown in grey. Plot from ref. [17].

will be mounted back-to-back in strings through a single-arm lock system. This consists of a single holder system made of low background copper and silicon plates.

The commissioning of the Phase II upgrade is currently ongoing and the starting of data taking is foreseen in 2014.

5. – Conclusions

The background level in GERDA Phase II will be a factor about ten times lower than in Phase I, *i.e.* BI $\simeq 10^{-3}\,\mathrm{cts}/(\mathrm{keV\,kg\,yr})$. Thanks to the increased mass of enriched germanium an exposure of 100 kg yr will be reached in about 3 years. The corresponding sensitivity on the half-life of $0\nu\beta\beta$ decay is about $T^{0\nu}_{1/2} \simeq 1.4 \cdot 10^{26}$ yr.

REFERENCES

[1] The GERDA Collaboration, *Letter of Intent* (2004).
[2] The GERDA Collaboration, *Proposal*, `http://www.mpi-hd.mpg.de/GERDA` (2004).
[3] Klapdor-Kleingrothaus H. V. *et al.*, *Eur. Phys. J. A*, **12** (2001) 147.
[4] Alseth C. E. *et al.*, *Phys. Rev. D*, **65** (2002) 092007.
[5] Klapdor-Kleingrothaus H. V. *et al.*, *Phys. Lett. B*, **586** (2004) 198.
[6] Klapdor-Kleingrothaus H. V. and Krivosheina I. V., *Mod. Phys. Lett. A*, **21** (2006) 1547.
[7] Schwingenheuer B., *Ann. Phys. (N.Y.)*, **525** (2013) 269.
[8] Gando A. *et al.*, *Phys. Rev. Lett.*, **110** (2013) 062502.
[9] Auger M. *et al.*, *Phys. Rev. Lett.*, **109** (2012) 032505.
[10] The GERDA Collaboration, *Phys. Rev. Lett.*, **111** (2013) 122503.
[11] The GERDA Collaboration, *Eur. Phys. J. C*, **73** (2013) 2330.
[12] Klapdor-Kleingrothaus H. V. *et al.*, *Nucl. Instrum. Methods A*, **481** (2002) 149.
[13] Ashitkov V .D. *et al.*, *Instrum. Exp. Tech.*, **46** (2003) 153.
[14] Agostini M. *et al.*, *J. Instrum.*, **6** (2011) P08013.
[15] The GERDA Collaboration, *J. Phys. G: Nucl. Part. Phys.*, **40** (2013) 035110.
[16] The GERDA Collaboration, *Eur. Phys. J. C*, **74** (2014) 2764.
[17] The GERDA Collaboration, *Eur. Phys. J. C*, **73** (2013) 2583.
[18] C. Macolino on behalf of the GERDA Collaboration, *Mod. Phys. Lett. A*, **29** (2014) 1430001.
[19] Caldwell A. and Kröninger K., *Phys. Rev. D*, **74** (2006) 092003.
[20] Caldwell A., Kollar D. and Kröninger K., *Comput. Phys. Commun.*, **180** (2009) 2197.
[21] Bhupal Dev P. S. *et al.*, *Phys. Rev. D*, **88** (2013) 091301.
[22] Kotila J. and Iachello F., *Phys. Rev. C*, **85** (2012) 034316.
[23] Rodriguez T. R. and Martinez-Pinedo G., *Phys. Rev. Lett.*, **105** (2010) 252503.
[24] Menendez J. *et al.*, *Nucl. Phys. A*, **818** (2009) 139.
[25] Barea J., Kotila J. and Iachello F., *Phys. Rev. C*, **87** (2013) 014315.
[26] Suhonen J. and Civitarese O., *Nucl. Phys. A*, **847** (2010) 207.
[27] Meroni A., Petcov S. T. and Simkovic F., *JHEP*, **1302** (2013) 25.
[28] Simkovic F., Rodin V., Faessler A. and Vogel P., *Phys. Rev. C*, **87** (2013) 045501.
[29] Mustonen M. T. and Engel J., *Phys. Rev. C*, **87** (2013) 064302.
[30] Smolnikov A. and Grabmayr P., *Phys. Rev. C*, **81** (2010) 028502.
[31] Budjáš D. *et al.*, *J. Instrum.*, **8** (2013) P04018.
[32] Andreotti E. *et al.*, *J. Instrum.*, **8** (2013) P06012.